Polypyrrole/MWCNT-*gr*-PSSA Composite for Flexible and Highly Conductive Transparent Film

Tae Hwan Lim,[1] Kyung Wha Oh,[2] Seong Hun Kim[1]

[1]*Department of Organic and Nanoengineering, Hanyang University, Sungdong-Gu, Seoul 133-791, Korea*
[2]*Department of Home Economics Education, Chung-Ang University, Dongjak-Gu, Seoul 156-756, Korea*

Received 20 August 2010; accepted 10 March 2011
DOI 10.1002/app.34507
Published online 27 July 2011 in Wiley Online Library (wileyonlinelibrary.com).

ABSTRACT: This study compares the properties of a highly conductive polymer based on polypyrrole and multiwall carbon nanotubes (MWCNTs) grafted with poly (styrenesulfonic acid) (PPy/MWCNT-*gr*-PSSA) prepared for flexible indium tin oxide-free organic solar cell (OSC) anode with those of PH500 poly(3,4-ethylenedioxythiophene) : poly(styrenesulfonate) (PEDOT : PSS) in various solvents. Hydrophilic poly(styrenesulfonic acid) (PSSA) was grafted on the MWCNT surfaces to improve dispersion of the MWCNT in an aqueous solution. MWCNT-*gr*-PSSA was added because MWCNT acts as a conductive additive and a template for the polymerization of PPy. Polymerization yields increased as the amount of MWCNT-*gr*-PSSA increased and reached a maximum when 50% of MWCNT-*gr*-PSSA was added. The conductivity of PPy/MWCNT-*gr*-PSSA composite was further improved and the value reached $\sim$ 152 S/cm with the addition of a toluenesulfonic acid (TSA)/HCl dopant mixture. To prepare a flexible OSC anode, PPy/MWCNT-*gr*-PSSA dissolved in solvent mixture, was coated onto a polyethylene terephthalate (PET) substrate. PPy/MWCNT-*gr*-PSSA was dissolved in a mixture of solvents including DMSO, NMP, EG, DEG, and glycerol of a high boiling point that was spin coated onto the PET, then annealed for 30 min at various temperatures. The conductivity of PPy/MWCNT-*gr*-PSSA was further enhanced with solvent treatment and annealing at temperature ranges of 100–175°C. Under optimum conditions, the conductivity and transmittance of PPy/MWCNT-*gr*-PSSA on PET reached 602 S/cm and 84% at 550 nm, respectively. In addition, it was confirmed that the energy level and mechanical strength of the film were suitable for OSC electrode use. © 2011 Wiley Periodicals, Inc. J Appl Polym Sci 123: 388–397, 2012

Key words: organic solar cells; anode; polypyrrole; MWCNT; conductivity

INTRODUCTION

Organic polymer based solar cells (OSCs) have attracted attention because of their potential for solving future energy crises, low cost, and a variety of photovoltaic applications. Recent improvements in the efficiency of OSCs are impressive. A bulk heterojunction (BHJ) and tandem layer was substituted for a planar heterojunction photoactive layer divided into an electron–donor and acceptor surface that had a significant influence on the efficiency enhancement.[1,2] Generally, the BHJ layer of polymer-based OSCs is composed of a combination of poly(3-hexylthiophene) (P3HT) and 1-(3-methoxycarbonyl)-propyl-1-phenyl-(6,6)C_{61} (PCBM) produced by spin coating. These OSCs provide the highest efficiency of up to 4–5% through the thermal annealing conditions and solvent evaporation time.[3–5] Silicon-based solar cells and dye-sensitized solar cells have an efficiency $\sim$ 25 and 10% higher than that of OSCs. Despite their relatively low efficiency, compared with inorganic solar cells, polymer-based OSCs are very attractive in terms of their potential for a roll-to-roll process, large area processing ability on flexible substrates, and cost-effective materials.[6,7] Most solar cell devices utilize indium tin oxide (ITO) as the hole collecting transparent conducting electrode material and poly(3,4-ethylenedioxythiophene) : poly(styrenesulfonate) (PEDOT : PSS) as the hole injection layer. ITO is generally processed at a high temperature to improve its conductivity and crystallinity on rigid substrates such as glass. However, under the numerous bending cycles on flexible substrates such as PET, the propagation of cracks occurs in ITO films that lead to considerable degradation of its conductivity and performance.[8] Moreover, the high cost of indium prevents large-scale use of ITO as a photovoltaic electrode compared with relatively low-cost polymer-based solar cells. Therefore, carbon nanotubes (CNT), graphene, metal grids, doped metal oxides, and organic polymers have been investigated to replace ITO with a flexible and transparent

Correspondence to: K. W. Oh (kwhaoh@cau.ac.kr).
Contract grant sponsor: The National Research Foundation of Korea; contract grant number: Project. 2010-0017228.

electrode.[9–13] One of the most recently examined materials of interest for organic-based electrodes is PEDOT : PSS because of its solution processability that makes it compatible with large scale usage concepts. PH500 (<1 S/cm) that is a commercial PEDOT : PSS dissolved in various solvents of a high boiling point. The conductivity of polymer electrode made of PH500 reached ~ 480 S/cm.[8,14,15] However, it is still a high-cost material and shows low conductivity on PET substrates compared with rigid substrates.[16]

This current study was to develop a low-cost, highly conductive, and flexible transparent film for OSC anodes. Polypyrrole (PPy) was selected for polymer electrode material substitute for PEDOT in our study because of its low cost and high conductivity. Multiwall carbon nanotubes (MWCNT) were chosen as a conductive additive and template to enhance its conductivity and thermal stability.[17,18] Grafting hydrophilic polymer, poly(styrenesulfonic acid) (PSSA) on the MWCNT surfaces was employed to improve dispersion in aqueous solutions because controlling the dispersion of MWCNT is very important for the development of high-performance polymer composite materials from among the various methods.[19] A flexible and highly conductive transparent film was fabricated by spin coating the synthesized PPy/MWCNT-*gr*-PSSA dissolved in organic polar solvents onto the substrate. The conductivity of these polymer composites was investigated according to the ratio of PPy : MWCNT-*gr*-PSSA and additional dopant treatment. Moreover, to develop good electrical and optical properties of film for OSC anodes, conductivity, transmittance and morphology were evaluated according to solid contents, spin rate, and annealing temperature to obtain optimum conditions. Finally, a band gap measurement and adhesiveness test were carried out to evaluate the suitability for a OSCs device.

EXPERIMENTAL

Materials

Pyrrole (reagent grade, 98%) was purchased from Aldrich. PH500 (CLEVIOS PH 500) was purchased from H. C. Starck. MWCNT was purchased from Il-jin Nanotech Co. (CM95, purity >95%, length 10–50 μm, diameter 10–30 nm). A 4-styrenesulfonic acid sodium salt hydrate (SSA^-Na^+, Sigma-Aldrich) was used as a grafting material. Ammonium persulfate (APS) and potassium persulfate ($K_2S_2O_8$) were used as a redox initiator and a radical initiator, respectively; both initiators were purchased from Sigma-Aldrich. The *p*-toluenesulfonic acid used as a dopant material was purchased from Sigma-Aldrich. ITO-coated glass (Aldrich, 15–25 Ω/sq) and ITO-coated PET (Fine Chemicals Industry, <35 Ω/sq) substrates were used for rigid and flexible ITO based devices, respectively. Marienfeld laboratory glassware was used as a pristine glass substrate. For increasing conductivity and thermal stability, various organic polar solvents and compounds were used. Dimethyl sulfoxide (DMSO), ethylene glycol (EG), diethylene glycol (DEG), and glycerol were purchased from Sigma-Aldrich and *N*-methyl-2-pyrrolidone (NMP) was purchased from Junsei Chemical Co.

MWCNT-*gr*-PSSA preparation

Pristine MWCNT contained impurities and amorphous carbon. There is strong van der Waals attraction between individual MWCNT that leads to aggregation and tangled networks. To enhance the dispersity of MWCNT, PSSA was grafted on the surface of MWCNT by radical polymerization.[20–23] $K_2S_2O_8$ (100 mg) and pristine MWCNT (100 mg) were introduced into a 500-mL round flask containing 250 mL distilled water. The dispersion was heated to 70°C with ultrasonication for 1 h. After SSA^-Na^+ was applied into the dispersion, polymerization was conducted under nitrogen purging for 24 h at 60°C. The weight ratio of $K_2S_2O_8$: MWCNT : SSA^-Na^+ was 1 : 1 : 50 according to previous research.[24] Polymerized MWCNT-*gr*-polystyrene sulfonate sodium (PSS^-Na^+) was washed with distilled water and methanol repeatedly to remove initiator, residual monomer, and PSS^-Na^+ homopolymer by centrifugation and microfiltration. Aggromerization of MWCNT-*gr*-PSS^-Na^+ was achieved with 5*M* HCl to protonate the sulfonate sodium salt to sulfonic acid. Modification of MWCNT by surface grafting was characterized by Fourier transfer infrared spectroscopy (FTIR), thermogravimetric analysis (TGA), and X-ray photoelectron spectroscopy (XPS).

In situ polymerization of pyrrole with MWCNT-*gr*-PSSA

Dried MWCNT-*gr*-PSSA powder was introduced into a round flask filled with water with ultrasonication. The dispersity of MWCNT-*gr*-PSSA in water was higher than that of pristine MWCNT and carboxylated MWCNT demonstrated in previous research.[17] Pyrrole monomer was dripped in the round flask containing well-dispersed MWCNT-*gr*-PSSA. PPy had been synthesized by *in situ* chemical oxidation polymerization, varying concentrations of pyrrole monomer, and APS from 40 to 95 wt % to observe the effect of PPy content on the conductivity of the composites.[25] Ten milliliters of the APS aqueous solution was injected for 10 h. The molar ratio of APS was the same as that of pyrrole monomer. The polymerization was conducted for 24 h at 5°C. *p*-Toluenesulfonic acid and HCl mixture was added

as a dopant to improve the conductivity of PPy/MWCNT-*gr*-PSSA. Polymerization of pyrrole with c-MWCNT was also conducted to compare with MWCNT-*gr*-PSSA.

Film preparation

PPy/MWCNT-*gr*-PSSA solid composites were dispersed in either pure water or a mixture of various solvents of high boiling point for spin coating onto the substrate. The solvent mixture was prepared by mixing DMSO, DEG, EG, and NMP in the same ratio. The solid content of PPy/MWCNT-*gr*-PSSA composites in the solvent mixture was varied from 0.75 up to 1.10 wt % to optimize conductivity and transmittance of the film. The solution was sonicated for 1 h and stirred at 500 rpm with a mechanical stirrer for an improved dispersion. The dispersion state was stable over 12 h without further stirring. Glycerol was finally mixed as a thermal stabilizer and binder to enhance the adhesive strength at a higher spin rate. PPy/MWCNT-*gr*-PSSA dissolved in solvent mixture was spin coated onto the substrate at various spin rates and annealed at different temperatures to determine the optimum conditions. Electrochemical and mechanical properties of prepared composite film were also evaluated for adaptation to a polymeric solar cell device.

Characterization

FTIR spectra (Nicolet 760 MAGNa-IR spectrometer) were used to define PSSA grafted on the pristine MWCNT. XPS (Axis NOVA, KRATOS) and TGA analysis (Perkin–Elmer, USA) was used to determine the amount of PSSA grafted onto MWCNT. The temperature was increased from 100 to 800°C at 20°C/min in nitrogen. SEM (JEOL JSM-6330F, Tokyo, Japan) was used to determine the morphology of the pristine MWCNT, c-MWCNT, and MWCNT-*gr*-PSSA. Conductivity was measured using a four-point probe method with a Keithley 238 high-current-source measuring unit and CMT-100*M* (Advanced Instrument Technology) at room temperature. The electrical conductivity was calculated using the Eq. (1) as follows[26]

$$\sigma\,(\mathrm{S/cm}) = \frac{\ln 2}{\pi \cdot t} \times \frac{I}{E} \approx 0.22/t \times \frac{I}{E} \qquad (1)$$

where E is the voltage drop across the inner probes; t is the thickness of the sample; I is the current passing through the outer probes; and σ is electrical conductivity. Optical properties were determined through UV–vis spectra (Scinco *S*-4100) to observe the transmittance of film. Film thickness and the surface images were measured using an AFM (Park Systems, XE-100). Band gap was measured by cyclic voltammetry (CV, 600D Series Electrochemical Workstation, CH Instruments, Inc.) method with Ag/Ag^+ as a reference electrode and coiled Pt wire as a counter electrode. 0.1*M* tetrabutylammonium perchlorate (TBAP) with acetonitrile was used as an electrolyte.

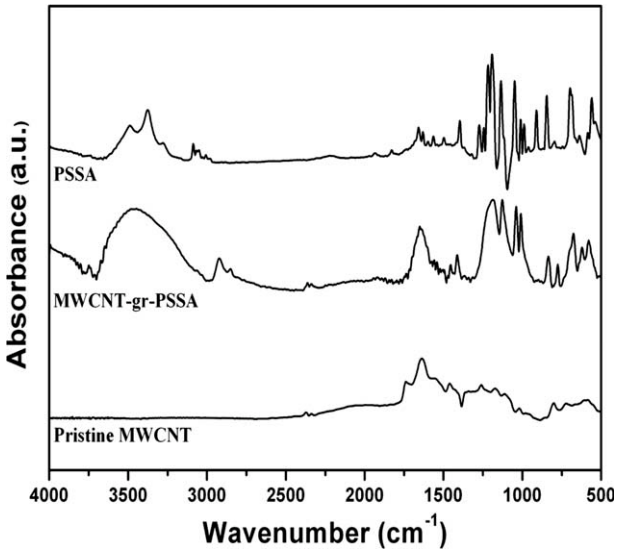

Figure 1 FT-IR spectra of pristine MWCNT, MWCNT-*gr*-PSSA, and PSSA homopolymer.

RESULTS AND DISCUSSION

MWCNT-*gr*-PSSA

To enhance the conductivity of a PPy-based anode in an OSC, MWCNT were selected as the most suitable template for this study. A novel surface modification technique of MWCNT grafting of hydrophilic polymer was introduced to improve dispersion of MWCNT in the water for a higher PPy polymerization yield. This surface grafting of MWCNT with hydrophilic polymer was also expected to provide additional benefits for the synthesis process and the product performance as compared with conventional acid treatment. PSSA was selected as a grafting hydrophilic polymer and the performance of MWCNT-*gr*-PSSA was compared with that of c-MWCNT produced by the conventional carboxylation of MWCNT through acid treatment with sulfuric acid and nitric acid (3 : 1) at 70°C for 24 h.[17] The surface of each MWCNT was expected to be modified chemically to produce hydrophilicity.

Figure 1 shows FTIR spectra of pristine MWCNT, MWCNT-*gr*-PSSA, and PSSA. The peaks at 1010 and 1040 cm^{-1} are due to the symmetric stretching of SO_2 from the sulfonyl group of PSSA. Asymmetric stretching of SO_2 on aromatic compounds produced strong peaks at 1140 and 1190 cm^{-1}. These peaks

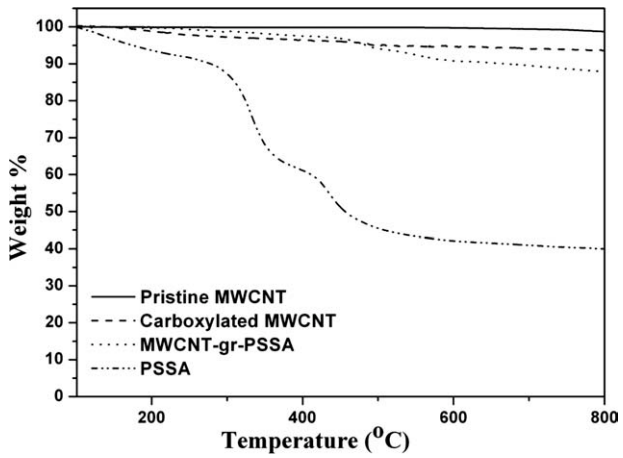

Figure 2 TGA thermograms of pristine MWCNT, carboxylated MWCNT, MWCNT-*gr*-PSSA, and PSSA homopolymer.

appeared as a doublet because sulfonic acid forms a resonance structure through electron stabilization and could be caused by the presence of a sulfonyl group from residual impurities such as $K_2S_2O_8$ or a homopolymer of PSSA. Therefore, MWCNT-*gr*-PSSA composite was treated with boiling water for 1 h to remove impurities. The intensity of each peak was almost the same after treatment with boiling water. These results ensured that PSSA was successfully grafted on the surface of MWCNTs.

TGA analysis was used to observe the amount of PSSA grafted on the MWCNT. As shown in Figure 2, three major weight loss temperatures appeared on the thermograms of PSSA homopolymer at 100–200°C, 300–350°C, and 400–450°C. These decompositions are expected to be caused by the evaporation of water and low molecular weight impurities, decomposition of sulfonyl groups on side chains, and main chain breakdown, respectively.[27] Accordingly, the major reason for thermal decomposition of MWCNT-*gr*-PSSA can be because of the grafted PSSA. Therefore, the amount of PSSA grafted on MWCNTs can be calculated from the weight loss of PSSA and MWCNT-*gr*-PSSA. From the thermograms in Figure 2, PSSA homopolymer and MWCNT-*gr*-PSSA show weight losses of 58.8% and 11.0%, respectively. MWCNTs do not show any obvious weight loss during the entire heating process. Therefore, the weight ratio of PSSA grafted on MWCNTs was expected to be $\sim$ 19 wt %.

The XPS analysis was measured to confirm that the MWCNT-*gr*-PSSA polymerized successfully and the quantitative analysis value was shown in Table I. The pristine MWCNT spectra exclusively exhibited O 1s and C 1s peaks. It reveals that the oxidation level of pristine MWCNT is very low. It was confirmed that the MWCNT used in our experiments had few functional groups. MWCNT-*gr*-PSSA and PSS-Na^+ were further investigated to analyze PSSA grafted ratios and confirm Na+ removed. In comparing the S 2p peak raw area of these materials, it was theorized that $\sim$ 18% PSSA was grafted onto the MWCNT surface and the value was almost similar with that measured by TGA. In addition, Na 1s peak was not observed in the MWCNT-*gr*-PSSA quantitative analysis. Based on the results, it was shown that PSS-Na+ was converted to PSSA successfully by protonating with HCl.

PPy/MWCNT-*gr*-PSSA

Pyrrole was selected for polymer electrode material in this research, because it is cheaper than EDOT for a PEDOT : PSS composite of commercial anode material and provides a similar conductivity and high thermal stability. In addition, MWCNTs were added to enhance the conductivity of PPy, because MWCNTs can act as a conductive agent and a template for the polymerization of PPy. Generally, while undoped PPy homopolymer exhibited in grain structure because of aggregation, PPy well dispersed by dopant or surfactant in a polymerization solution could be in the form of nanosized particles.[28,29] Thus, aqueous polymerization was conducted using MWCNT-*gr*-PSSA as a template for the synthesis of PPy. The performance of *in situ* polymerized PPy in presence of MWCNT-*gr*-PSSA was compared with that of PPy prepared with c-MWCNT. PPy was self-assembled in an interwoven structure with

TABLE I
Quantitative Analysis Values of Pristine MWCNT, MWCNT-*gr*-PSSA, and PSS^-Na^+ Homopolymer

Materials	Peak	Position BE (eV)	Raw area (cps)	Mass conc %	Atomic conc %
Pristine MWCNT	C 1s	280.690	516,494	98.63	98.97
	O 1s	526.690	14,482	1.37	1.03
MWCNT-*gr*-PSSA	C 1s	280.690	335,080	93.27	95.54
	O 1s	526.690	35,337	4.87	3.75
	S 2p	164.690	6,473	1.86	0.71
PSS^-Na^+	C 1s	280.690	117,828	49.09	61.94
	O 1s	526.690	122,958	25.34	24.01
	S 2p	164.690	34,878	15.03	7.10
	Na 1s	1068.690	63,362	10.54	6.95

TABLE II
Polymerization Yield According to the PPy Contents and Type of MWCNT Fabricated

Materials (content ratio, wt %)	Polymerization yield of PPy (%)
PPy/c-MWCNT[a] (50/50 wt %)	61.8
PPy/MWCNT-*gr*-PSSA[b] (95/5 wt %)	83.9
PPy/MWCNT-*gr*-PSSA (90/10 wt %)	83.8
PPy/MWCNT-*gr*-PSSA (80/20 wt %)	84.7
PPy/MWCNT-*gr*-PSSA (70/30 wt %)	88.4
PPy/MWCNT-*gr*-PSSA (60/40 wt %)	91.5
PPy/MWCNT-*gr*-PSSA (50/50 wt %)	95.5
PPy/MWCNT-*gr*-PSSA (40/60 wt %)	93.7

[a] PPy synthesized with carboxylated MWCNT using sulfuric and nitric acid.
[b] PPy synthesized with grafted MWCNT using PSSA.

MWCNT-*gr*-PSSA by chemical oxidative polymerization. PPy/MWCNT-*gr*-PSSA composites were synthesized at various pyrrole and MWCNT-*gr*-PSSA weight ratios to investigate optimum conditions for synthesis based on the polymerization yield and conductivity data.

As shown in Table II, the polymerization yield increased as the amount of MWCNT-*gr*-PSSA increased, to reach a maximum when 50% of MWCNT-*gr*-PSSA was added. However, when additional MWCNT-*gr*-PSSA was added, the polymerization yield decreased. As shown in Figure 3(b), conductivity values are also coincident with the polymerization yield. At an optimum ratio (5 : 5), PPy/MWCNT-*gr*-PSSA had the highest conductivity of $\sim$ 125 S/cm. This value is higher than those of both PPy/MWCNT doped with PSS (91 S/cm) and PPy/c-MWCNT (48 S/cm) as shown in Figure 3(a). This result represented that a well-dispersed MWCNT provided a beneficial influence on the conductivity of PPy/MWCNT composite.

The polymerization yield is also confirmed by the morphology of PPy/MWCNT composite as shown in Figure 4. Figure 4(a,b) showed PPy/c-MWCNT and PPy/MWCNT-*gr*-PSSA composites synthesized at the ratio of 5 : 5. The morphology of PPy/c-MWCNT [Fig. 4(a)] showed both aggregated PPy and separated c-MWCNTs that did not serve as a template for polymerization. On the other hand, PPy/MWCNT-*gr*-PSSA composites [Fig. 4(b)] showed that pyrroles were polymerized *in situ* on the surface of the well-dispersed MWCNT-*gr*-PSSA, increasing polymerization yield. With less MWCNT-*gr*-PSSA [Fig. 4(c,d)], homopolymer of PPy existed in an aggregated state because templates for the polymerization were not sufficiently provided. Therefore, the polymerization yield decreased as shown in Table II.

For the further enhancement of conductivity, a mixture of TSA/HCl was used as a dopant because it was proven that a mixture of TSA/HCl dopants enhanced conductivity.[29] The molar ratio of PPy and TSA/HCl was 2 : 1 and the polymerization was performed at 5°C for 2 h. As shown in Figure 3(a), the conductivity of PPy/MWCNT-*gr*-PSSA composite polymerized with TSA/HCl dopant was further improved and the value reached $\sim$ 152 S/cm.

Effect of solvents and annealing temperature

Many theoretical studies have been conducted to enhance conductivity by using organic polar solvents.[30–34] According to previous research,[30–34] organic solvents and compounds with two or more polar groups influence conductivity. These materials lead to conformational change of the PEDOT chains and the mechanism is similar to secondary doping. Because EDOT has a large dipole moment (μ = 1.87 D)

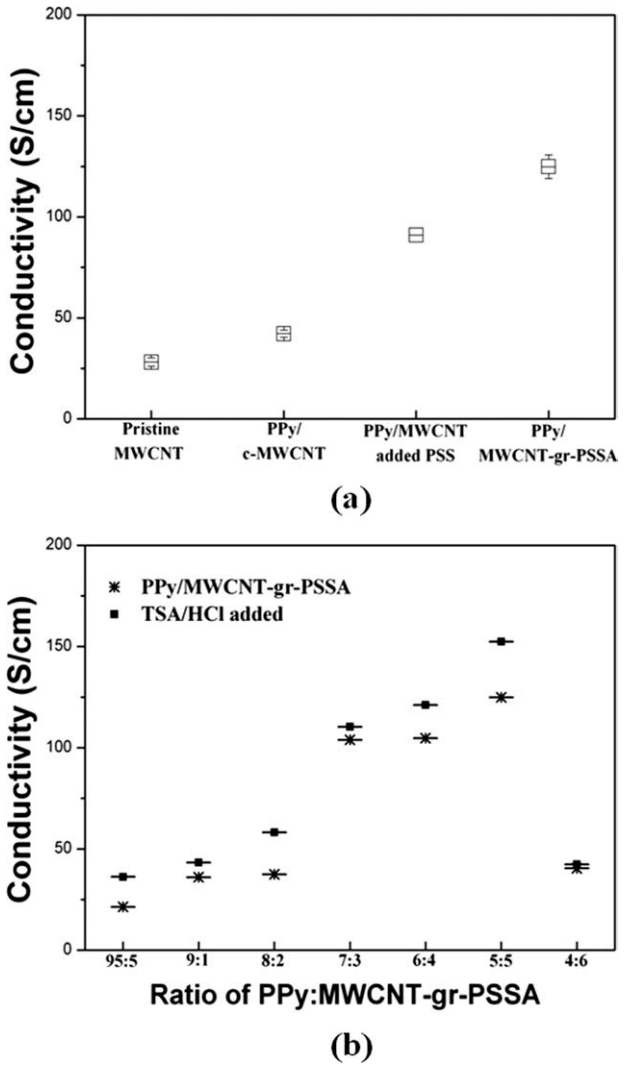

Figure 3 (a) Conductivity of pristine MWCNT, PPy/c-MWCNT, PPy/MWCNT doped with PSS, and PPy/MWCNTgr-PSSA. (b) Effect of the ratio of PPy : MWCNT-*gr*-PSSA and TSA/HCl dopant on the conductivity of PPy/MWCNT-*gr*-PSSA composites.

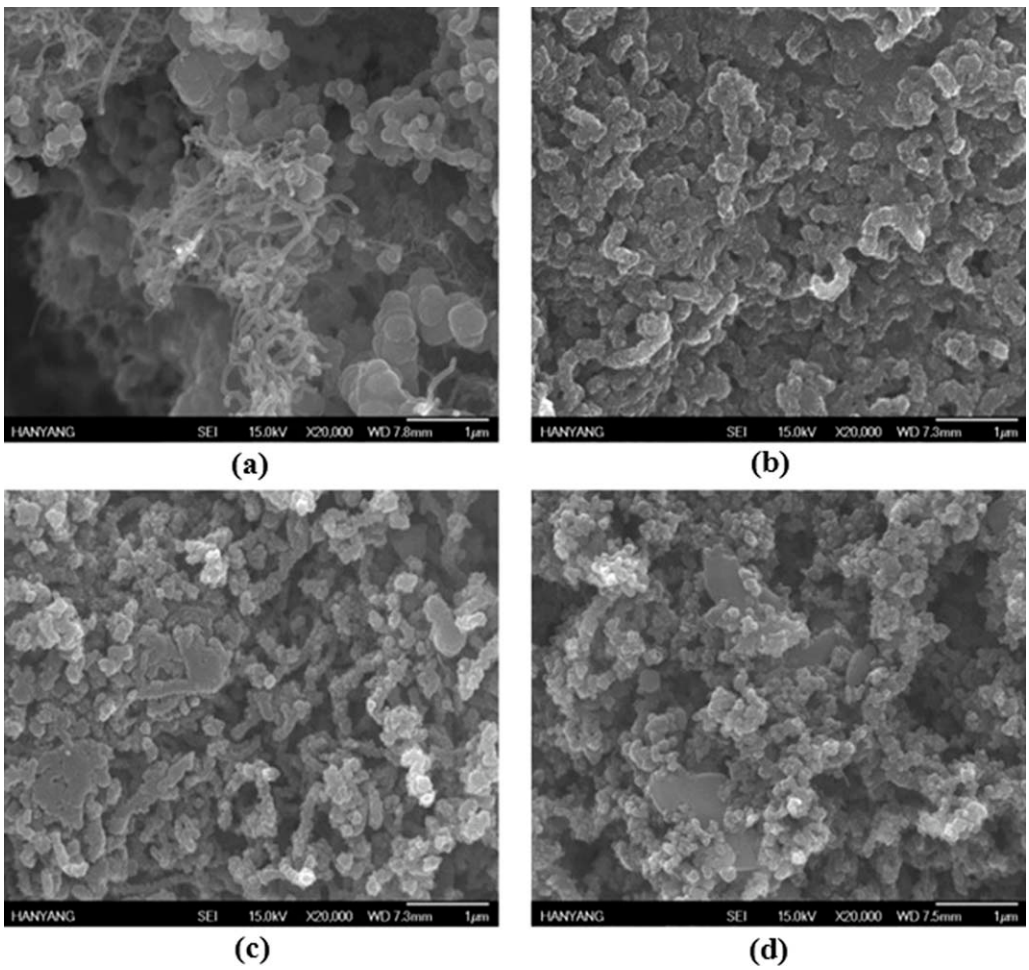

Figure 4 SEM images of (a) PPy/c-MWCNT composite (5 : 5) and PPy/MWCNT-*gr*-PSSA composites of various ratios; (b) 5 : 5, (c) 7 : 3, and (d) 9 : 1.

and PSS chains formed hydrogen bonds, a strong interaction between PEDOT : PSS and organic polar compounds was easily maintained. Pyrrole has a similar dipole moment ($\mu = 1.80$ D) to EDOT and PSSA as well as formed strong hydrogen bonds; therefore, PPy/MWCNT-*gr*-PSSA was expected to be modified by these solvents.

PPy/MWCNT-*gr*-PSSA composite should be dispersed in either an aqueous solution or some kind of solvent for spin coating on the substrate. Because PSSA is a hydrophilic polymer, PPy/MWCNT-*gr*-PSSA composite can be dispersed in an aqueous solution. However, aqueous state materials are assumed to provide relatively low conductivity and poor morphology. Therefore, we selected several solvents of a high boiling point to improve conductivity and the toleration of high temperature treatment. A mixture of various polar solvents such as NMP, DMSO, EG, DEG, and glycerol of the same weight ratio were used to enhance conductivity, because these solvents can induce a secondary doping effect by conformational change of the polymer chains. As a result, the conductivity of PPy/MWCNT-*gr*-PSSA composites coated on the glass substrate improved from 24 to 320 S/cm after solvent treatment at room temperature. Moreover, the increased conductivity by solvent treatment can also be explained by changes in the surface morphologies of the film.[30–34] As shown in Figure 5, the surface morphology of film prepared with PPy/MWCNT-*gr*-PSSA dissolved in solvent mixture was smoother than that coated with PPy/MWCNT-*gr*-PSSA aqueous solution. Root-mean-square roughness of film coated with PPy/MWCNT-*gr*-PSSA in solvent mixture (average, 0.129 nm) is less than that coated with PPy/MWCNT-*gr*-PSSA aqueous solution (Rq : average, 0.555 nm). This finding is consistent with previous research,[16,35,36] which revealed that the surface of solvent-treated film after heating was much smoother; in addition, this morphological change induced an increase in conductivity.

After PPy/MWCNT-*gr*-PSSA composites were dissolved in solvent mixture and spin coated at 2000 rpm for 30 s onto a glass substrate, they were annealed for 30 min at various temperatures. The effects of different annealing temperatures on the

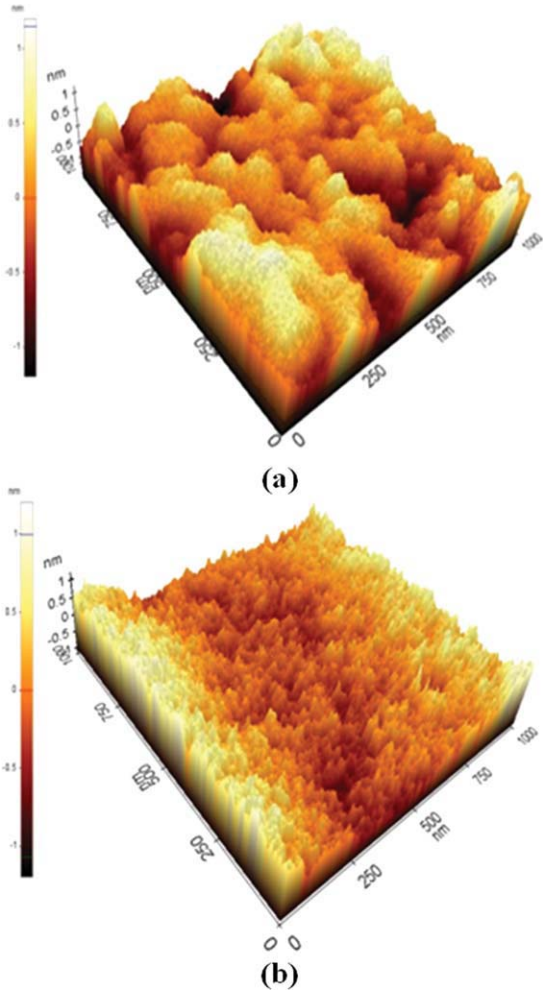

Figure 5 AFM images (1 × 1 μm) of (a) aqueous PPy/MWCNT-*gr*-PSSA film and (b) solvent-modified PPy/MWCNT-*gr*-PSSA film. [Color figure can be viewed in the online issue, which is available at wileyonline library.com.]

conductivity of PPy/MWCNT-*gr*-PSSA film are shown in Figure 6. The conductivity of these films was significantly improved by an annealing treatment as compared with that of films dried at room temperature (~ 320 S/cm). The conductivity changed with annealing temperature, and the highest conductivity (~ 606 S/cm) was observed at temperatures in the range of 100–175°C. However, the conductivity continuously decreased as the annealing temperature increased over 175°C. This result is because of solvent evaporation and thermal degradation of the PPy/MWCNT-*gr*-PSSA film.[37] The conductivity value is maintained for temperatures up to 175°C because most solvents have high boiling points of ~ 170–190°C. According to previous studies,[30–34] organic solvents such as glycerol, NMP, DMSO, and DMF improve conductivity by a secondary doping effect through chemical and physical structural changes of the polymer chain; in addition, this effect is optimized during heat treatment.

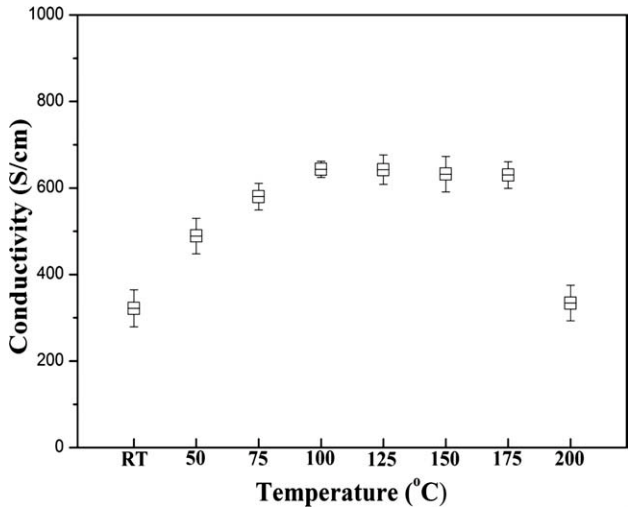

Figure 6 Effect of annealing temperature on the conductivity of PPy/MWCNT-*gr*-PSSA films when they were treated for 30 min (Solid content: 0.9 wt %).

Film properties

Because one of the major properties of OSC anodes is film transparency and high conductivity, spin coating conditions were optimized by varying the solid content and spin rate. As shown in Figures 7 and 8, the conductivity increased but transmittance decreased as the solid content increased. Considering the conductivity and transparency of films, 0.9 wt % solid content was selected as an optimum condition. Under this condition, the conductivity of PPy/MWCNT-*gr*-PSSA coated film was 606 S/cm and its transmittance was 84% at 550 nm.

Transmittance relies on the thickness of film according to the spin rate. Figure 9 shows the effect of spin rate on the transmittance and conductivity of films. Generally, the transmittance of films increased

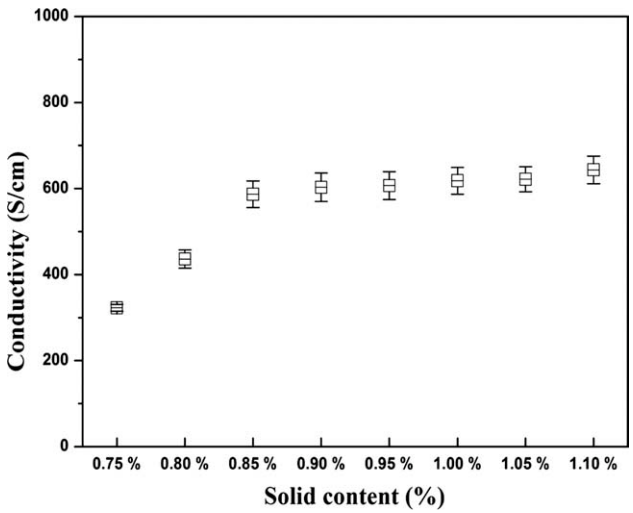

Figure 7 Effect of solid content on the conductivity of solvent-modified PPy/MWCNT-*gr*-PSSA film.

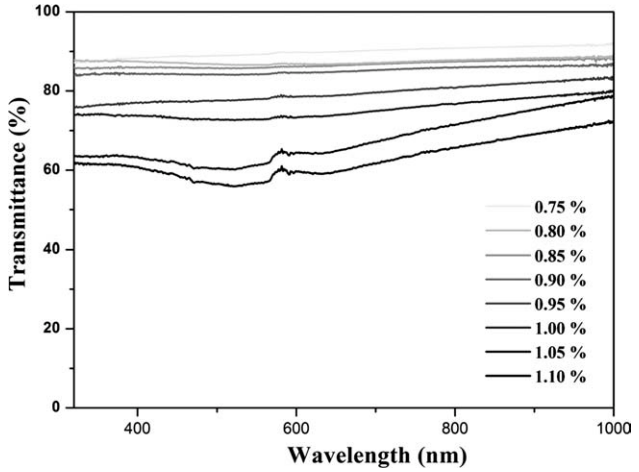

Figure 8 Effect of solid content on the optical transmittance of solvent-modified PPy/MWCNT-*gr*-PSSA film.

with the decreasing film thickness without significant changes in film conductivity. The thickness of film spin coated at 3000 rpm was 180 nm as measured by AFM. The transmittance value of this film was on average 88% at 550 nm. The film thickness measured was 270 nm at 2000 rpm and 410 nm at 500 rpm. Their average transmittance was 84 and 59%, respectively. Conductivity was approximately the same at 606 S/cm up to 2000 rpm. With additional increases in spin rate, the conductivity decreased to 510 S/cm at 3000 rpm. Therefore, considering both conductivity and transparency, PPy/MWCNT-*gr*-PSSA anode film for the OSCs was prepared at 2000 rpm and its properties were compared with those of previously developed anode materials.

The transmittance and conductivity of PH500 spin coated at 2000 rpm were 77% at 550 nm and 480 S/cm,

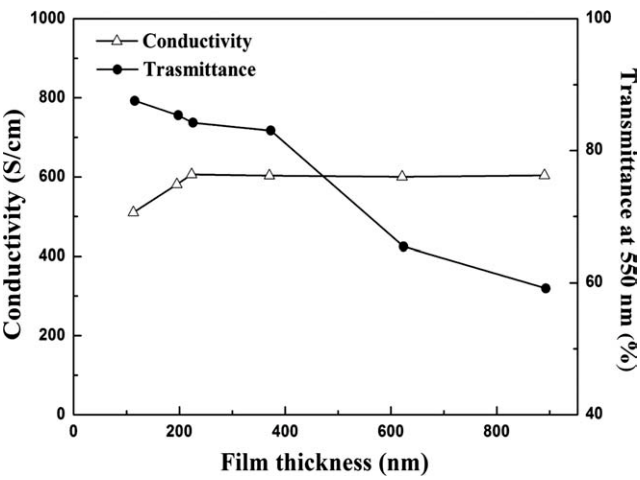

Figure 9 Effect of the spin rate on the conductivity and transmittance properties of solvent-modified PPy/MWCNT-*gr*-PSSA film (solid content: 0.9 wt %; annealing temperature: 125°C).

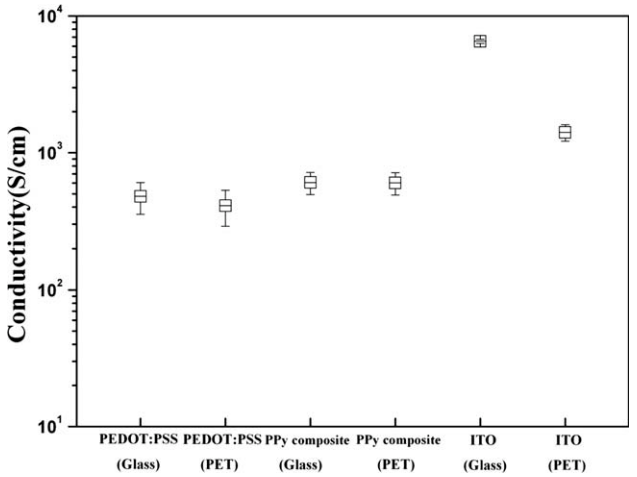

Figure 10 Effect of substrate materials on the conductivities of coated PEDOT : PSS, PPy/MWCNT-*gr*-PSSA, and ITO.

respectively. The transmittance and conductivity of PPy/MWCNT-*gr*-PSSA film spin coated at 2000 rpm were 84% at 550 nm and 606 S/cm, respectively. Therefore, it was confirmed that both transmittance and conductivity of PPy/MWCNT-*gr*-PSSA film, that were major factors applying to OSC anodes, were superior to those of PEDOT : PSS film.

For flexible OSCs, a PET substrate was introduced as a substitute for a glass substrate. The properties of film coated onto the PET substrate were measured and compared with that of glass substrate. Figure 10 showed the conductivities of ITO, PEDOT : PSS, and PPy/MWCNT-*gr*-PSSA film coated on glass and PET substrate, respectively. PEDOT : PSS and ITO on the PET had lower conductivity than those on glass substrate. The conductivity of PEDOT : PSS and ITO on the PET substrate was decreased to 410 and 1410 S/cm, respectively. These values were significantly lower than those for glass substrate. However, the conductivity of PPy/MWCNT-*gr*-PSSA film did not significantly change regardless of a substrate of $\sim$ 602 S/cm. Therefore, the PPy/MWCNT-*gr*-PSSA film prepared in this study is considered a good potential material for flexible OSC anodes.

Electrochemical and adhesive properties

Electrochemical and mechanical properties evaluated the suitability of PPy/MWCNT-*gr*-PSSA film for a OSCs device. The band gap was measured to present the electrochemical properties of the electrode since the electrical energy gap between the HOMO and LUMO of the electrode determined the OSCs device structure. The cyclic voltammograms shown in Figure 11 were recognized as an easy and effective method to evaluate the band gap of the polymer electrode. The onset potential method was used to

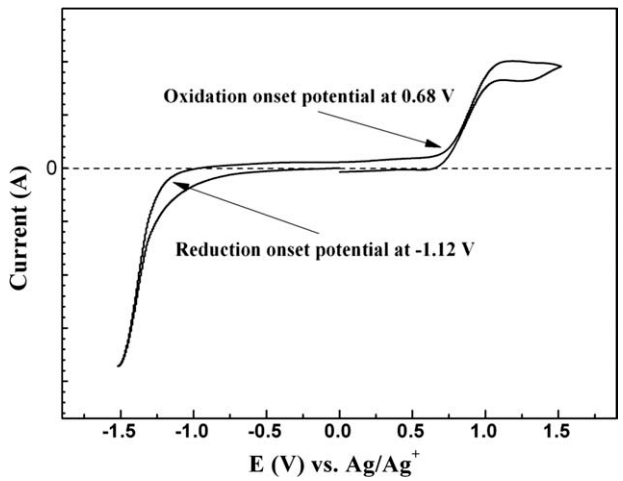

Figure 11 Cyclic voltammograms of Solvent modified PPy/MWCNT-*gr*-PSSA film at the scan rate of 20 mV/s.

calculate the band gap from previous research.[38] The band gap was calculated using the Eq. (2) as follows, where I_p is the ionization potential, E_a is the electron affinity, E_{ox} is the onset oxidation potentials, and E_{red} is onset reduction potentials.

$$\begin{aligned} I_p &= -(E_{ox} + 4.4)\ \text{eV} \\ E_a &= -(E_{red} + 4.4)\ \text{eV} \\ E_g(\text{Energy band gap}) &= I_p - E_a \end{aligned} \tag{2}$$

E_{ox} and E_{red} were 0.68 V and −1.12 V, and, I_p and E_a were −5.08 and −3.28 eV, respectively. Therefore, the band gap of PPy/MWCNT-*gr*-PSSA film is 1.80 eV because these values were equal to HOMO and LUMO energy levels. Although the band gap of PPy/MWCNT-*gr*-PSSA film is higher than PEDOT : PSS (1.5–1.6 eV) and its HOMO energy level was lower than ITO (−4.70 eV), the energy level of this electrode was appropriate to effectively transfer the electron because the HOMO level was higher than that of the P3HT : PCBM photoactive layer (<−5.10 eV). Therefore, PPy/MWCNT-*gr*-PSSA film is suitable for a OSCs device.

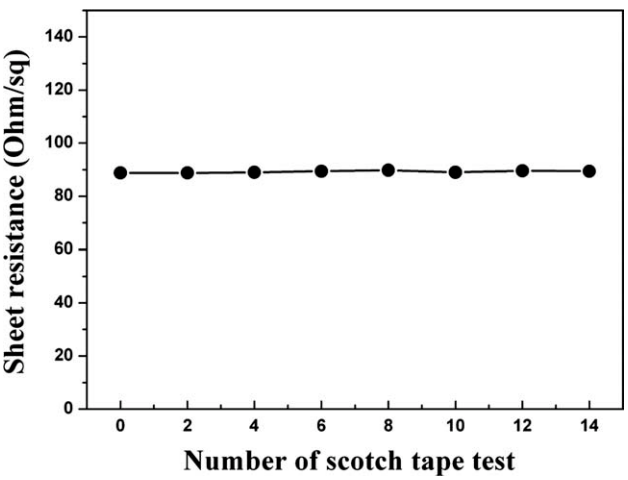

Figure 12 Effect of a multiple scotch tape detaching test on the sheet resistance of PPy composite film.

A scotch tape test estimated the adhesiveness of PPy/MWCNT-*gr*-PSSA film to the substrate by the previous method.[39] The electrical properties of PPy/MWCNT-*gr*-PSSA film were measured after a repeated scotch tape detachment and the results are shown in Figure 12. Sheet resistance values were maintained from 88.8 to 89.4 Ω/sq after 14 cycles. In addition, a stripped area on the surface was rarely observed after multiple testing. Based on the results of the scotch tape test, it was theorized that PPy composite film on a flexible substrate was suitable for an adapting electrode.

CONCLUSIONS

Highly effective polymer based OSC anodes composed of PPy/MWCNT-*gr*-PSSA were prepared in this study. It was confirmed that PSSA grafting on the MWCNT surface has a good effect on improving the dispersion of the MWCNT in an aqueous solution. MWCNT-*gr*-PSSA acts as an additive and template for the polymerization of PPy, and the maximum polymerization yield was obtained when 50% of MWCNT-*gr*-PSSA was added. The conductivity of PPy/MWCNT-*gr*-PSSA composite was further improved by the addition of a TSA/HCl dopant mixture. It was confirmed that added mixture led to secondary doping with PPy/MWCNT-*gr*-PSSA. After solvent modification and annealing, the conductivity and transmittance of PPy/MWCNT-*gr*-PSSA-coated PET film reached 602 S/cm and 84% at 550 nm, respectively. These values are higher than those of PEDOT : PSS coated PET film. It was confirmed that the energy level of PPy/MWCNT-*gr*-PSSA film was appropriate for the effective transfer of an electron since the band gap was 1.80 eV and its HOMO level was higher than that of the P3HT : PCBM photoactive layer (<−5.10 eV). This level of PPy/MWCNT-*gr*-PSSA film is a good match to that of the photoactive layer for efficient electron and hole transport. Sheet resistance was maintained after multiple adhesiveness tests. Therefore, the overall results revealed that PPy/MWCNT-*gr*-PSSA on PET film had good potential as a flexible OSC anode material.

References

1. Chen, J.; Cao, Y. Acc Chem Res 2009, 42, 1709.
2. Hadipour, A.; Boer, B. D.; Wildeman, J.; Kooistra, F. B.; Hummelen, J. C.; Turbiez, M. G. R.; Wienk, M. M.; Janssen, R. A. J.; Blom, P. W. M. Adv Funct Mater 2006, 16, 1897.
3. Ma, W.; Yang, C.; Gong, X.; Lee, K.; Heeger, A. J Adv Funct Mater 2005, 15, 1617.
4. Li, G.; Shrotriya, V.; Huang, J.; Yao, Y.; Moriarty, T.; Emery, K.; Yang, Y. Nature Mater 2005, 4, 864.

5. Reyes, M. R.; Kim, K. K.; Carroll, D. L. Appl Phys Lett 2005, 87, 083506.
6. Krebs, F. C. Solar Energy Mater Solar Cells 2009, 93, 1636.
7. Krebs, F. C. Org Electron 2009, 10, 761.
8. Na, S. I.; Kim, S. S.; Jo, J.; Kim, D. Y. Adv Mater 2008, 20, 4061.
9. Rowell, M. W.; Topinka, M. A.; McGehee, M. D.; Prall, H. J.; Dennler, G.; Sariciftci, N. S.; Hu, L.; Gruner, G. Appl Phys Lett 2006, 88, 233506.
10. Wu, J.; Becerril, H. A.; Bao, Z.; Liu, Z.; Chen, Y.; Peumans, P. Appl Phys Lett 2008, 92, 263302.
11. Xie, Z.; Hung, L. S.; Zhu, F. Chem Phys Lett 2003, 381, 691.
12. Owen, J.; Son, M. S.; Yoo, K. H.; Ahn, B. D.; Lee, S. Y. Appl Phys Lett 2007, 90, 033512.
13. Ouyang, J.; Chu, C. W.; Chen, F. C.; Xu, Q.; Yang Y. Adv Funct Mater 2005, 15, 203.
14. Hau, S. K.; Yip, H. L.; Zou, J.; Jen, A. K. Y. Org Electron 2009, 10, 1401.
15. Du, H.; Reinhard, M.; Vogeler, H.; Puetz, A.; Klein, M. F. G.; Schabel, W.; Colsmann, A.; Lemmer U. Thin Solid Films 2009, 517, 5900.
16. Zhou, Y.; Zhang, F.; Tvingstedt, K.; Barrau, S.; Li, F.; Tian, W.; Inganas, O. Appl Phys Lett 2008, 92, 233308.
17. Kim, D. K.; Oh, K. W.; Kim, S. H. J Polym Sci Part B: Polym Phys 2008, 46, 2255.
18. Sharma, R. K.; Karakoti, A.; Seal, S.; Zhai, L. J Power Sources 2010, 195, 1256.
19. Spitalsky, Z.; Tasis, D.; Papagelis, K.; Galiotis, D. Prog Polym Sci 2010, 35, 357.
20. Qin, S.; Qin, D.; Ford, W. T.; Herrera, J. E.; Resasco, D. E.; Bachilo, S. M.; Weisman, R. B. Macromolecules 2004, 37, 3965.
21. Shaffer, M. S. P.; Koziol, K.; Chem Commun 2005, 2074.
22. Hirsch, A. Angew Chem Ed 2002, 41, 1853.
23. Tessier, L.; Chancolon, J.; Alet, P. J.; Trenggono, A.; Deniau, G.; Jegou, P.; Palacin, S. Phys Stat Sol 2008, 205, 1412.
24. Kim, D. K.; Oh, K. W.; Kim, S. H. Mol Cryst Liq Cryst 2009, 510, 51.
25. Wu, T. M.; Chang, H. L.; Lin, Y. W. Comp Sci Tech 2009, 69, 639.
26. Kaufmann, E. N.; Characterization of Materials, Vol. 1; New York: Wiley-Interscience; 2003, ISBN: 0–471-26882–8.
27. Patel, R.; Im, S. J.; Ko, Y. T.; Kim, J. H.; Min, B. R. J Indust Eng Chem 2009, 15, 299.
28. Oh, K. W.; Park, H. J.; Kim, S. H. J Appl Polym Sci 2004, 91, 3659.
29. Kim, D. K.; Oh, K. W.; Ahn, H. J.; Kim, S. H. J Appl Polym Sci 2008, 107, 3925.
30. Ouyang, J.; Xu, Q.; Chu, C. W.; Yang, Y.; Li, G.; Shinar, J. Polymer 2004, 45, 8443.
31. Zhang, F.; Johansson, M.; Andersson, M. R.; Hummelen, J. C.; Inganas, O. Adv Mater 2002, 14, 662.
32. Huang, J.; Miller, P. F.; Wilson, J. S.; Mello, A. J.; Mello, J. C.; Bradley, D. D. C. Adv Funct Mater 2005, 15, 290.
33. Kim, J. Y.; Jung, J. H.; Lee, D. E.; Joo, J. Synth Met 2002, 126, 311.
34. Crispin, X.; Jakobsson, F. L. E.; Crispin, A.; Grim, P. C. M.; Andersson, P.; Volodin, A.; Haesendonck, C. V.; Auweraer, M. V. D.; Salaneck, W. R.; Berggren, M. Plastic Electrodes Chem Mater 2006, 18, 4354.
35. Somboonsub, B.; Invernale, M. A.; Thongyai, S.; Praserthdam, P.; Scola, D. A.; Sotzing, G. A. Polymer 2010, 51, 1231.
36. Jonsson, S. K. M.; Birgerson, J.; Crispin, X.; Greczynski, G.; Osikowicz, W.; van der Gon, A. W. D.; Salaneck, W. R.; Fahlman, M. Synth Met 2003, 139, 1.
37. Singh, R.; Narula, A. K.; Tandon, R. P.; Rao, S. U. M.; Panwar, V. S.; Mansingh, A.; Chandra, S. Synth Met 1996, 79, 1.
38. Cervini, R.; Li, X. C.; Spencer, G. W. C.; Holmes, A. B.; Moratti, S. C.; Friend, R. H. Synth Met 1997, 84, 359.
39. Wei, Y.; Yeh, J. M.; Jin, D.; Jia, X.; Wang, J. Chem Mater 1995, 7, 969.